ACS OMEGA

Article

Cite This: ACS Omega 2019, 4, 10975−10984

http://pubs.acs.org/journal/acsodf

Thermal Stability and Flame Retardancy Properties of Epoxy Resin Modified with Functionalized Graphene Oxide Containing Phosphorus and Silicon Elements

Maoyong Zhi, Quanyi Liu,* Hao Chen, Xiantao Chen, Sihai Feng, and Yuanhua He*

College of Civil Aviation Safety Engineering, Civil Aviation Flight University of China, Deyang 618307, People's Republic of China

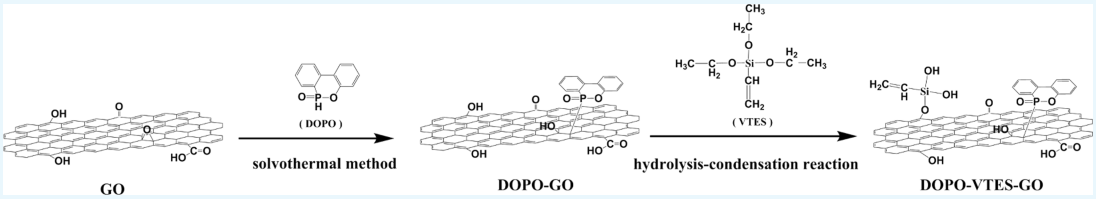

ABSTRACT: Phosphorus- and silicon-modified graphene oxide was prepared to improve the thermal stability and flame retardancy properties of epoxy resin. 9,10-Dihydro-9-oxa-10-phosphaphenanthrene-10-oxide (DOPO) and vinyltriethoxysilane (VTES) were successfully grafted onto the surface of graphene oxide (GO) through solvothermal synthesis and hydrolysis−condensation reaction, respectively. Subsequently, the functionalized graphene oxide grafted by DOPO and VTES (DOPO−VTES−GO) was incorporated into the epoxy resin by the solution blending method. The effect of DOPO−VTES−GO on the thermal stability and flame-retardant properties of epoxy resin was systematically studied. Thermogravimetric analysis showed that the thermal stability and char residue yield of DOPO−VTES−GO/epoxy were increased obviously compared with those of pure epoxy resin and DOPO−GO/epoxy. Cone calorimeter test results showed that DOPO−VTES−GO/epoxy had better flame retardancy than pure epoxy resin and DOPO−GO/epoxy on reducing the peak of heat release rate, total heat release, and total smoke production. Furthermore, the char residue after the cone calorimeter tests was investigated by scanning electron microscopy−energy-dispersive X-ray spectrometry, Raman spectroscopy, and Fourier transform infrared measurements. These results demonstrated that the DOPO−VTES−GO can enhance the graphitization degree of char residues and promote the formation of the thermally stable char. In addition, the mechanism of flame retardancy was proposed, and DOPO−VTES−GO exerts the synergistic effect mainly by means of catalytic charring in the condensed phase and capturing hydroxyl or hydrogen radicals from thermal decomposition of epoxy resin in the gas phase. This work provides novel insights into the preparation of phosphorus−silicon−graphene oxide ternary synergistic flame retardants for thermosetting polymer materials.

1. INTRODUCTION

Epoxy resin, as one of the major conventional thermosetting resins, has wide industrial applications including adhesives,[1] coatings,[2] electronics,[3] aerospace parts,[4] and marine systems,[5] owing to its excellent mechanical strength, superior adhesion, good solvent resistance, and thermal insulation.[6] However, high flammability has significantly restricted its potential applications. Therefore, it is necessary to reduce the flammability of epoxy resin.[7] Many researchers are devoted to improving the flame retardancy performance of epoxy through the synthesis of inherently flame-retardant epoxy resin and/or the addition of flame retardants in the epoxy matrix.[8,9] Among these flame-retardant systems, halogen-containing flame retardants have been extensively studied to endow flame retardancy of epoxy resins.[10] Unfortunately, the toxic and corrosive gases released by halogenated flame retardants during combustion are very harmful to the environment and human health.

Graphene is becoming an attractive halogen-free flame retardant for epoxy resin due to its two-dimensional carbon layer structure as a physical barrier to slow the escape of the volatile products.[11] However, flame retardancy is not yet satisfactory by adding individual graphene into the polymer matrix because of its combustibility in the air atmosphere.[12] 10-Dihydro-9-oxa-10-phosphaphenanthrene-10-oxide (DOPO) is a highly effective phosphorus-based flame retardant due to its high thermal stability and good oxidation resistance.[13] Therefore, the synergistic flame retardancy effect of graphene and DOPO is desirable to overcome this problem.[14−16] Liao et al.[15] reported that DOPO has been grafted onto the surface of reduced graphene oxide (rGO) to develop a synergistic DOPO−rGO flame retardant, and the addition of DOPO−rGO improves the thermal stability and limiting oxygen index of epoxy resin. Luo et al.[16] developed DOPO−rGO by grafting DOPO onto the surface of GO, then used it as a flame retardant to improve the flame retardancy of epoxy resin, and the result showed that the heat release rate and total heat release (THR) of epoxy filled with DOPO−rGO were dramatically decreased compared with pure epoxy,

Received: March 27, 2019
Accepted: June 12, 2019
Published: June 24, 2019

DOI: 10.1021/acsomega.9b00852
ACS Omega 2019, 4, 10975−10984

Scheme 1. Schematic Illustration of the Preparation Process for the DOPO−VTES−GO Flame Retardant

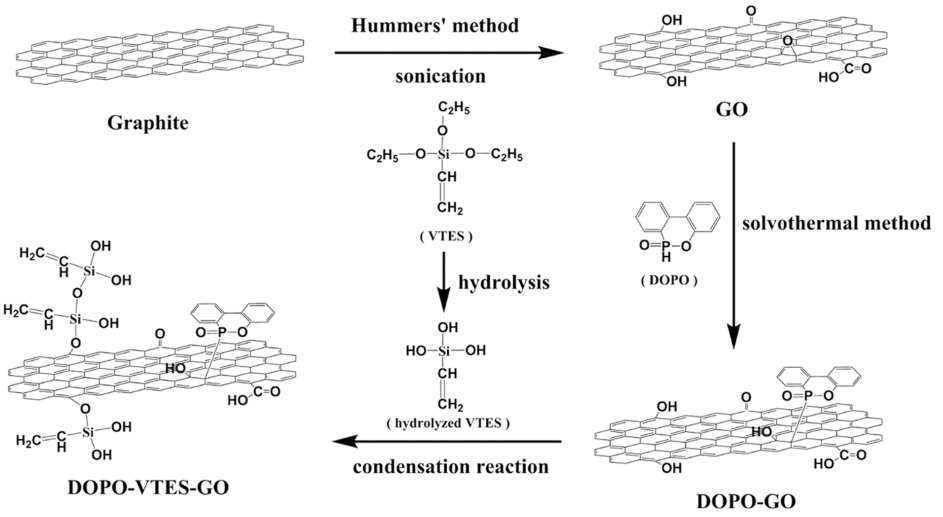

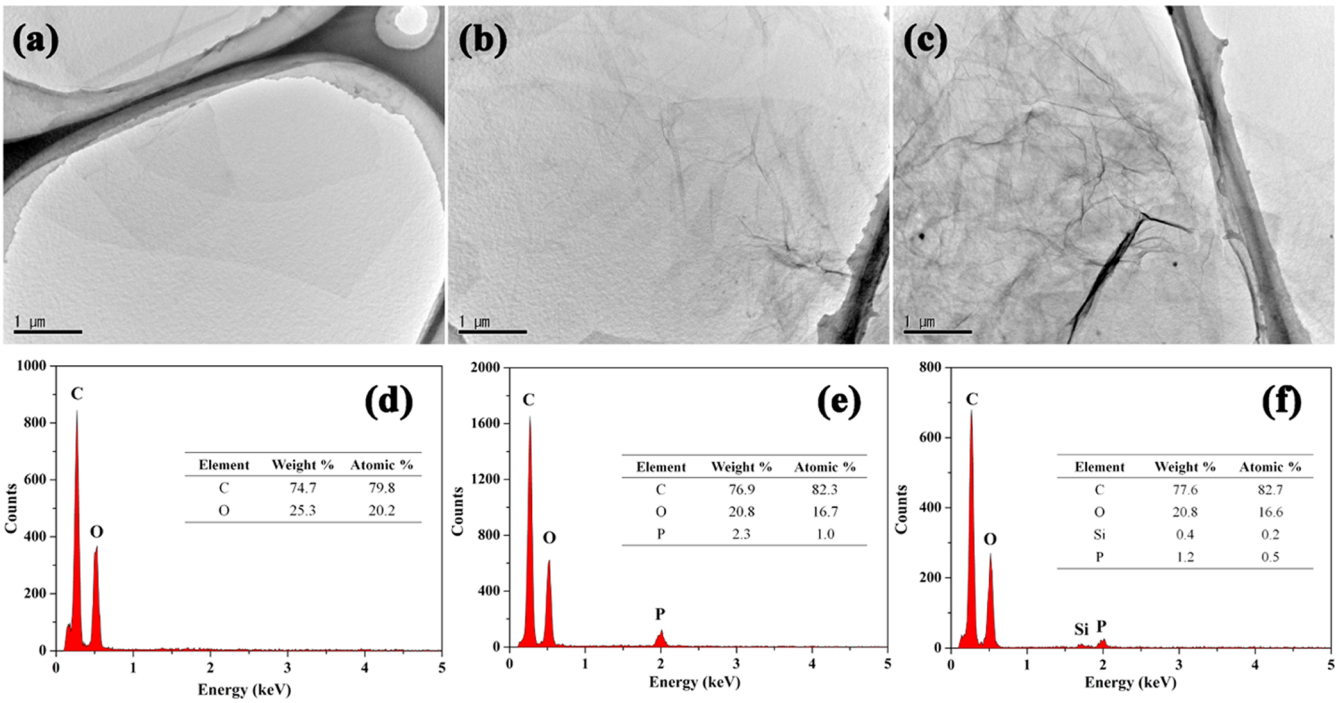

Figure 1. TEM images of the (a) GO, (b) DOPO−GO, and (c) DOPO−VTES−GO, and the corresponding EDX spectra of (d) GO, (e) DOPO−GO, and (f) DOPO−VTES−GO.

indicating that DOPO−rGO could impart better flame-retardant properties to epoxy resin.

Unfortunately, both oxygen-containing groups on the surfaces of graphene oxide and phosphorus−oxygen groups in the DOPO tend to decompose earlier than epoxy resin during combustion, which seriously reduces the thermal stability of epoxy resin.[17] To overcome these drawbacks, surface modification of GO has drawn the attention of many researchers. Wang et al.[18] synthesized a novel graphene-based hybrid consisting of graphene and nanosilica to alleviate the thermal-oxidation degradation of the graphitic structure. The hybrid can be transformed into silica nanosheets with high resistance to oxidative degradation at high temperature, which can delay the thermal degradation of the polymer chain segments during the combustion process. However, the effect of the graphene-based hybrid flame retardant on smoke production of epoxy resin during combustion has not been studied. Qian et al.[19] prepared a novel flame-retardant additive by reacting rGO with (3-isocyanatopropyl)triethoxysilane and DOPO via a sol−gel process, which exhibited a significant improvement in the thermal stability and flame retardancy of epoxy resin. Unfortunately, the synthesis process of the flame retardant was a complex and time-consuming process.

In this work, we developed an effective synthesis method for the functionalized graphene oxide containing phosphorus and silicon elements. The functionalized graphene oxide with DOPO and vinyltriethoxysilane (DOPO−VTES−GO) was synthesized by a solvothermal method and the following hydrolysis−condensation reaction approach. In the solvothermal process, DOPO was grafted onto GO through the

DOI: 10.1021/acsomega.9b00852
ACS Omega 2019, 4, 10975−10984

chemical reaction of the P−H group with the epoxy groups. In the subsequent hydrolysis−condensation process, the reaction between the −Si−OH group of hydrolyzed VTES and hydroxyl groups of GO happened. Transmission electron microscopy−energy-dispersive X-ray spectrometry (TEM−EDS) and Fourier transform infrared (FTIR) spectroscopy confirmed the successful grafting of the DOPO and VTES onto the surface of GO. The thermal stability and flame retardancy properties of the DOPO−VTES−GO/epoxy composite were investigated by means of thermogravimetric analysis (TGA) and limiting oxygen index and cone calorimeter tests. Moreover, the flame retardancy mechanism was explored by the aid of scanning electron microscopy−energy-dispersive X-ray spectrometry (SEM−EDS), Raman spectroscopy, and FTIR analysis.

2. RESULTS AND DISCUSSION

2.1. Characterization of DOPO−GO and DOPO−VTES−GO Flame Retardants. As illustrated in Scheme 1, in the reaction process for the surface grafting of VTES on the GO surface, there are two main steps: (1) VTES hydrolysis to produce hydrolyzed VTES in acid solution, (2) hydroxyl groups of hydrolyzed VTES can react with hydroxyl groups on the surface of GO nanosheets through the condensation reaction process. Besides, the self-condensation reaction happens between hydrolyzed VTES grafted on the GO surface and free hydrolyzed VTES to form siloxane or poly(siloxane) bonds. TEM measurements have been conducted to investigate the morphologies of the GO, DOPO−GO, and DOPO−VTES−GO, as shown in Figure 1a−c, respectively. GO exhibits a crumpled nanostructure with very thin features, and most parts of the GO sheets are very smooth (Figure 1a). However, the morphologies of DOPO−GO and DOPO−VTES−GO show rough surfaces, as shown in Figure 1b,c, respectively. It is obvious that pebblelike DOPO nanoparticles are homogeneously decorated on the GO surface. After the surface grafting of VTES on the GO surface, there are many poly(siloxane) bonds on the GO surface due to the self-condensation reaction of hydrolyzed VTES. Previous studies have shown that hydrogen bonding can be formed to produce silane nanoballs when two poly(silanol) rings are close to each other,[20] and silica nanoballs were synthesized using organo-silane precursors.[21,22] The GO nanosheets can provide reaction sites for the formation of silane nanoballs. For the TEM image of DOPO−VTES−GO (Figure 1c), it can be seen that a few silane nanospheres are distributed on the surface of GO.

It can also be easily observed that amounts of small balls are uniformly dispersed on the surface of DOPO−VTES−GO. EDS analyses revealed the elemental compositions of the GO, DOPO−GO, and DOPO−VTES−GO, as shown in Figure 1d−f, respectively. In Figure 1d, it can be seen that the contents of carbon and oxygen are 74.7 wt % and 25.3 wt % in the GO, respectively. The existence of oxygen is attributed to the oxygen-containing groups on the surface of GO. As shown in Figure 1e, the DOPO−GO contains C, O, and a small number of P, indicating that DOPO was grafted onto the surface of GO. The grafting ratio of DOPO on the surface of GO was calculated as 16.0 wt %. In addition, Figure 1f displays that Si element is detected in DOPO−VTES−GO, and the weight percentages of C, O, P, and Si were 77.6, 20.8, 1.2, and 0.4 wt %, respectively. The presence of P and Si elements confirmed the successful grafting of DOPO and VTES onto the surface of GO.

FTIR spectra are often employed to confirm the presence of characteristic functional groups. Figure 2 shows the FTIR

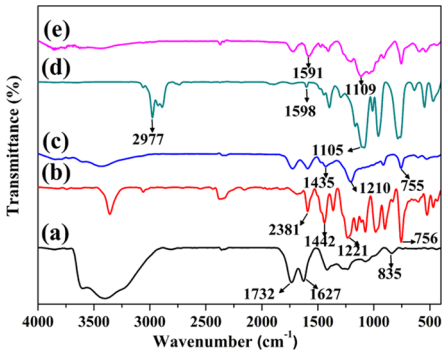

Figure 2. FTIR spectra of (a) GO, (b) DOPO, (c) DOPO−GO, (d) VTES, and (e) DOPO−VTES−GO.

spectra of GO, DOPO, DOPO−GO, VTES, and DOPO−VTES−GO. It can be seen in Figure 2a that the absorption peaks at 3300−3500 cm^{-1} (the O−H stretching vibration of −OH groups), 1732 cm^{-1} (the C═O stretching vibration of carboxyl groups and carbonyl groups), 1627 cm^{-1} (the stretching vibration of sp^2 hybridized carbon), and 835 cm^{-1} (C−O vibrations of epoxy groups) reveal typical characteristic functional groups of GO.[23] From the spectrum of DOPO (Figure 2b), the bands at 2381, 1442, 1221, and 756 cm^{-1} were assigned to the stretching vibrations of the P−H, P−Ph, P═O, and P−O−Ph, respectively. The FTIR spectrum from the DOPO−GO (Figure 2c) exhibited three characteristic peaks at 1435, 1210, and 755 cm^{-1}, indicating the presence of the P−Ph, P═O, and P−O−Ph, respectively. It was also observed that the peak intensity of the epoxy groups for DOPO−GO decreased significantly, and the P−H group disappeared, which proved the successful grafting of DOPO onto GO through the chemical reaction of the P−H group with the epoxy ring and carbonyl groups. In Figure 2d, several characteristic peaks of the VTES groups appeared at the bands of 2977 cm^{-1} (C−H vinyl stretching), 1598 cm^{-1} (C═C stretching), and 1080 cm^{-1} (Si−O−C stretching), which was in agreement with the previous report.[24] Additionally, it can be seen that several absorption peaks at 1591 and 1108 cm^{-1} appear in the spectrum of DOPO−VTES−GO, which are attributed to the C═C stretching vibrations and Si−O−C stretching vibrations, respectively.[25] Meanwhile, the typical hydroxyl group peak at 3300−3500 cm^{-1} becomes very weak, suggesting that the reaction between the −Si−OH group of hydrolyzed VTES and hydroxyl groups of GO happens. These results suggested that GO was successfully grafted by DOPO and VTES (Table 1).

The thermal stability of the samples was systematically investigated by TG analysis under the nitrogen atmosphere, as shown in Figure 3. The initial decomposition temperature (T_{on}, 5% weight loss), the maximum degradation rate temperature (T_{max}), and the char residue at 700 °C are obtained from the TG and differential thermogravimetry (DTG) curves and listed in Table 2. As presented in Figure 3 and Table 2, it can be observed that GO is not thermally stable and the main weight loss of GO was found at 150−300 °C because of the decomposition of labile oxygen-containing

DOI: 10.1021/acsomega.9b00852
ACS Omega 2019, 4, 10975−10984

Table 1. Formulas of the Cured Pure Epoxy and Epoxy Composites

sample	epoxy (g)	DDM (g)	GO (g)	DOPO (g)	DOPO−GO (g)	DOPO−VTES−GO (g)
pure epoxy	60	20	0	0	0	0
GO/epoxy	60	20	3	0	0	0
DOPO/epoxy	60	20	0	3	0	0
DOPO−GO/epoxy	60	20	0	0	3	0
DOPO−VTES−GO/epoxy	60	20	0	0	0	3

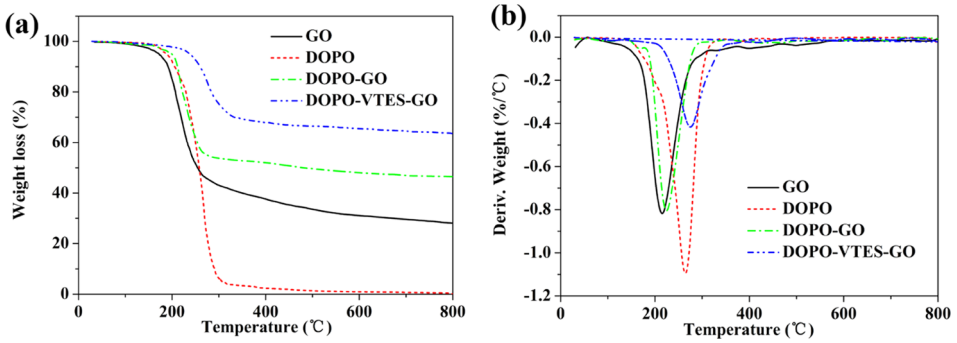

Figure 3. (a) TG and (b) DTG curves of GO, DOPO, DOPO−GO, and DOPO−VTES−GO.

Table 2. TGA and Limiting Oxygen Index (LOI) Data of the Samples

sample	T_{on} (°C)	T_{max} (°C)	char yield at 700 °C (wt %)	LOI (%)
GO	172	216	29.6	
DOPO	188	264	0.71	
DOPO−GO	199	224	46.9	
DOPO−VTES−GO	238	275	64.5	
pure epoxy	352	388	17.2	19.7
GO/epoxy	341	381	19.4	22.3
DOPO/epoxy	335	379	20.7	23.5
DOPO−GO/epoxy	343	382	24.5	24.7
DOPO−VTES−GO/epoxy	345	386	30.2	27.5

functional groups. Compared to GO, T_{on} of DOPO−GO slightly increased (from 172 to 199 °C), and the char yield of DOPO−GO is higher (from 29.6 to 46.9 wt %), which may be attributed to thermal decomposition of phosphorus-containing functional groups in the early stages and condensed phase activity.[26] After functionalization of GO by DOPO and VTES, many thermally labile oxygen functional groups were removed, and the T_{on} and T_{max} of DOPO−VTES−GO were much higher than those of GO. The TG curve of DOPO−VTES−GO also proves that DOPO and VTES have been successfully grafted on the surface of GO, which is consistent with the result of the TEM−EDS and FTIR measurements.

2.2. Thermal Stability Properties of Epoxy Composites. The effect of GO, DOPO, DOPO−GO, and DOPO−VTES−GO on the thermal stability of epoxy resin was also studied by TG analysis, as presented in Figure 4 and Table 2. The thermal decomposition process of epoxy resin has one stage as the pure epoxy. The T_{on} and T_{max} of pure epoxy are 352 and 388 °C, respectively. It is found that the incorporation of 5 wt % GO in epoxy decreased T_{on} and T_{max} by ca. 11 and 7 °C, respectively, in comparison with that of pure epoxy. The worse thermal stability might be because the GO loading decreases the cross-link density of the epoxy. DOPO−GO/epoxy displays a more effective improvement in the char residue from 17.2 to 24.5 wt %, than that of GO/epoxy composite (19.4 wt %), which is mainly due to the char-forming catalytic effect of phosphates.[27,28] It is noticeable that the T_{on} and T_{max} of the DOPO−VTES−GO/epoxy composite are 345 and 386 °C, respectively, which are close to the values of the pure epoxy. In addition, the char yield of 5 wt % DOPO−VTES−GO/epoxy was remarkably increased to 30.2 wt %. which is higher than those of 1.5 wt % nanosilica−GO/epoxy composite (14.2 wt %)[18] and 5 wt % flame retardants (FRs−rGO)/epoxy composite (19.6 wt %).[19] This is mainly attributed to the synergistic effect of phosphorous and silicon

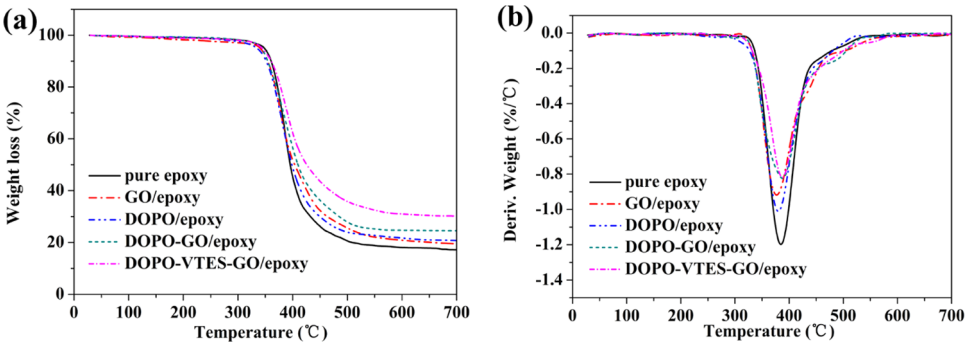

Figure 4. (a) TG and (b) DTG curves of pure epoxy and its composites.

DOI: 10.1021/acsomega.9b00852
ACS Omega 2019, 4, 10975−10984

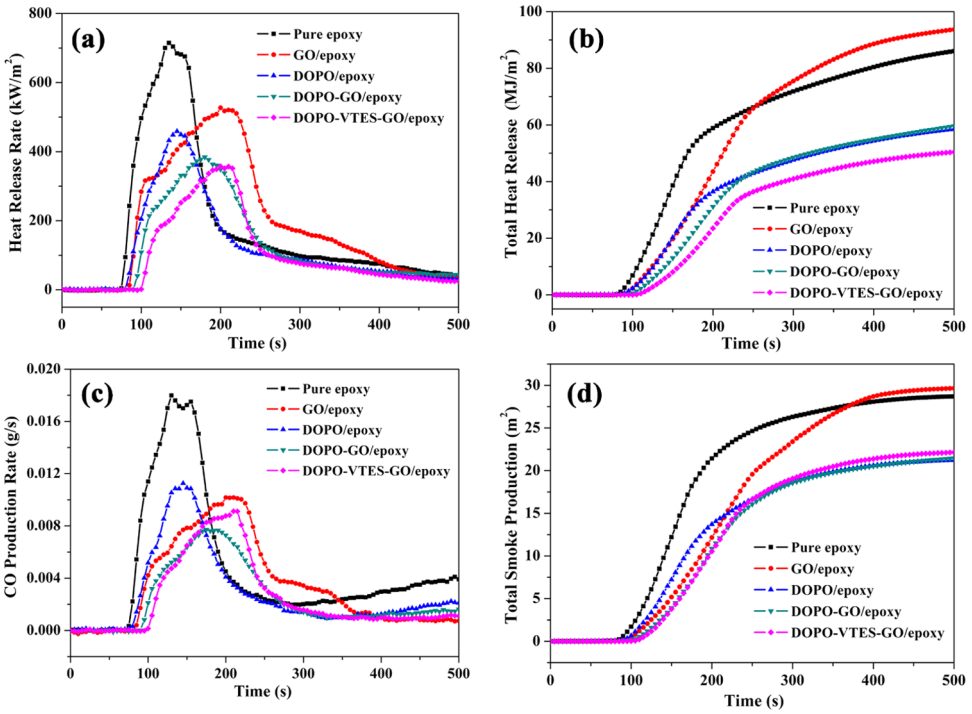

Figure 5. (a) HRR, (b) THR, (c) CO production rate, and (d) TSP curves of pure epoxy and its composites.

Table 3. Cone Calorimeter Results of Pure Epoxy and Its Composites

sample	TTI (s)	PHRR (kW m^{-2})	t_{PHRR} (s)	FIGRA (kW m^{-2} s^{-1})	THR (MJ m^{-2})	AEHC (MJ kg^{-1})	TSP (m^2)
pure epoxy	87	714.7	135	5.3	86.1	15.94	28.6
GO/epoxy	88	526.8	200	2.6	93.8	16.01	29.8
DOPO/epoxy	86	458.6	145	3.2	58.5	13.73	21.3
DOPO−GO/epoxy	102	384.1	180	2.1	59.6	14.97	21.8
DOPO−VTES−GO/epoxy	106	390.3	200	1.9	50.5	14.68	18.3

elements, where phosphorous accelerates the formation of char and silicon enhances the thermal stability of the char during the thermal degradation process of epoxy resin.[29]

2.3. Flame Retardancy Performance of Epoxy Composites. Limiting oxygen index and cone calorimeter tests are effective methods to evaluate the flame-retardant properties of polymeric materials during combustion.[30] Therefore, limiting oxygen index and cone calorimeter tests were adopted to investigate the combustion behavior of pure epoxy and its composites.

The LOI values of pure epoxy and its composites are given in Table 2. As shown in Table 2, the LOI value of pure epoxy was only 19.7%, and it was easy to burn. The LOI value of GO/epoxy composite showed a slight increase, which is likely attributed to the physical barrier effect of GO to inhibit the heat and mass transfer process.[31] Obviously, it was found that the LOI value of the DOPO−GO/epoxy composite was increased to 24.7%, suggesting a good synergistic effect between DOPO and GO. This finding is consistent with the previous research work.[15] Moreover, as for the DOPO−VTES−GO/epoxy composite, the LOI value was improved significantly from 24.7 to 27.5% in comparison with the DOPO−GO/epoxy composite. Therefore, DOPO−VTES−GO exhibits a better flame-retardant effect than DOPO−GO, which is probably because the formation of silicon dioxide with high thermal stability enhances the thermal oxidative stability of the char layer.[30] In our previous experimental research on the limiting oxygen index test of epoxy composites, the LOI value of DOPO−VTES−GO/epoxy composites increased monotonically with DOPO−VTES−GO content, but it was found that the LOI value showed almost no increase when DOPO−VTES−GO content was more than 5 wt %. Therefore, the appropriate addition of DOPO−VTES−GO is 5 wt % in the DOPO−VTES−GO/epoxy composite.

The heat release rate, total heat release, CO production, and total smoke production curves of pure epoxy and its composites are shown in Figure 5. Besides, the selected data obtained from cone calorimeter tests are summarized in Table 3, including time to ignition (TTI), peak heat release rate (PHRR), time to peak heat release (t_{PHRR}), fire growth rate index (FIGRA), total heat release (THR), average of effective heat of combustion (AEHC), and total smoke production (TSP). TTI is an important index to evaluate the combustion performance of materials, which can be determined by the onset of a heat release rate curve.[32] As listed in Table 3, compared to pure epoxy, the TTI of DOPO−VTES−GO/epoxy was significantly prolonged, which would be beneficial for effective escape and firefighting.[33] As shown in Figure 5a and Table 3, it can be observed that that pure epoxy burns very rapidly after ignition and the PHRR value is 714.7 kW m^{-2}, which demonstrates the flammability of pure epoxy. The PHRR values of GO/epoxy and DOPO/epoxy decrease to 526.8 and 458.6 kW m^{-2}, respectively. With the incorporation of DOPO−GO, the PHRR for DOPO−GO/epoxy was further

DOI: 10.1021/acsomega.9b00852
ACS Omega 2019, 4, 10975−10984

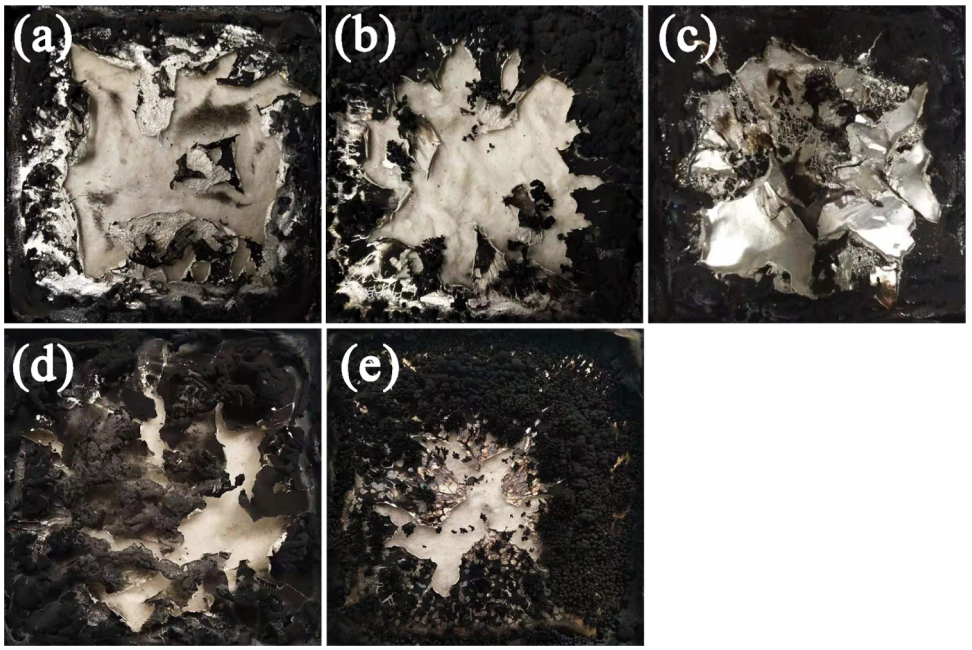

Figure 6. Digital photographs of char residues after cone calorimeter tests of (a) pure epoxy, (b) GO/epoxy, (c) DOPO/epoxy, (d) DOPO−GO/epoxy, and (e) DOPO−VTES−GO/epoxy.

decreased to 384.1 kW m^{-2}, suggesting the synergistic effect of GO and DOPO on the inhibition of HRR. In addition, the PHRR value of DOPO−VTES−GO/epoxy significantly decreased by 45.4% compared to the pure epoxy (from 714.7 to 390.3 kW m^{-2}), indicating the lowest fire hazards among these samples. Besides, the value (45.4%) is slightly higher than those of 4 wt % functionalized rGO/epoxy composite (37.7%),[12] 1.5 wt % nanosilica−GO/epoxy composite (39%),[18] and 5 wt % flame retardants (FRs−rGO)/epoxy composite (35%).[19]

The FIGRA implies the combustion propensity of a material in the fire, calculated from the ratio of PHRR and t_{PHRR},[34] and is presented in Table 3. With the addition of DOPO−VTES−GO, the FIGRA value of the epoxy composite is decreased by 64.1% compared to the pure epoxy (from 5.3 to 1.9 kW m^{-2} s^{-1}), indicating the delayed time to flashover and that it has earned precious time for evacuation and fire fighting.[35]

As illustrated in Figure 5b, the THR values of pure epoxy and its composites show a similar change trend as the PHRR. The THR value of DOPO−GO/epoxy composites is lower than those of pure epoxy, GO/epoxy, and DOPO/epoxy composites, which is attributed to the barrier effect of GO and catalytic carbonization of DOPO. Interestingly, the THR value of DOPO−VTES−GO/epoxy is lower than that of the DOPO−GO/epoxy composite and is reduced to 50.5 MJ m^{-2}, a 41.3% reduction compared to that of pure epoxy. In addition, the THR value of the DOPO−VTES−GO/epoxy composite is much higher than that (30.2%) of 4 wt % functionalized rGO/epoxy composite obtained by in situ polymerization.[12] This is mainly because that the high-temperature resistance effect of char residues was improved with addition of the silicon-containing flame retardant, which was in accordance with the TG results.

AEHC is defined as the ratio of the average heat release rate to the average mass loss rate from the cone calorimetry test, reflecting the degree of burning of volatile gases in gas-phase flame during combustion.[36] As shown in Table 3, it can be seen that the AEHC of GO/epoxy was almost the same as that of pure epoxy, indicating that GO did not play a role of a flame retardant in the gas phase. The AEHC of DOPO/epoxy obviously decreased with the addition of DOPO, indicating that DOPO exerted the flame-retardant effect in the gaseous phase. With the incorporation of other phosphorus-containing flame retardants, the AEHC of all of the epoxy composites showed a similar change. Also, the AEHC of the DOPO−VTES−GO/epoxy composite was approximately 8% lower than that of the pure epoxy.

Figure 5c shows the curves of the CO production rate of samples. It can be found that GO/epoxy can reduce the CO production rate compared with pure epoxy due to the barrier effect of GO. However, the CO production rate of DOPO/epoxy was slightly higher than that of pure epoxy, indicating that there was a catalytic effect of DOPO on the decrease of the CO production rate.[37] Moreover, the CO production rate of the DOPO−VTES−GO/epoxy composite was significantly decreased and lower than that of pure epoxy. The smoke production is also an important parameter to evaluate fire hazards and flame-retardant properties. It can be seen in Figure 5d and Table 3 that the TSP of DOPO−VTES−GO/epoxy was decreased by 36% compared with that of pure epoxy resin, indicating that DOPO−VTES−GO has a strong smoke suppression effect in epoxy composites. Based on the cone calorimeter analysis, it is worth noting that the trend of the cone calorimeter results is well consistent with the LOI results.

2.4. Analysis of Char Residues. As shown in Figure 6, the morphologies of char residues of pure epoxy and its composites after cone calorimeter tests were investigated by optical photographs. Obviously, it can be observed in Figure 6a that the char residue of pure epoxy is cracked and discontinuous and could not prevent combustible gas from escaping into the atmosphere. As indicated in Figure 6b,c, the char residue turns more homogeneous and compact with the incorporation of GO or DOPO in the epoxy matrix. Furthermore, it is clearly seen that the char residue of the

DOI: 10.1021/acsomega.9b00852
ACS Omega 2019, 4, 10975−10984

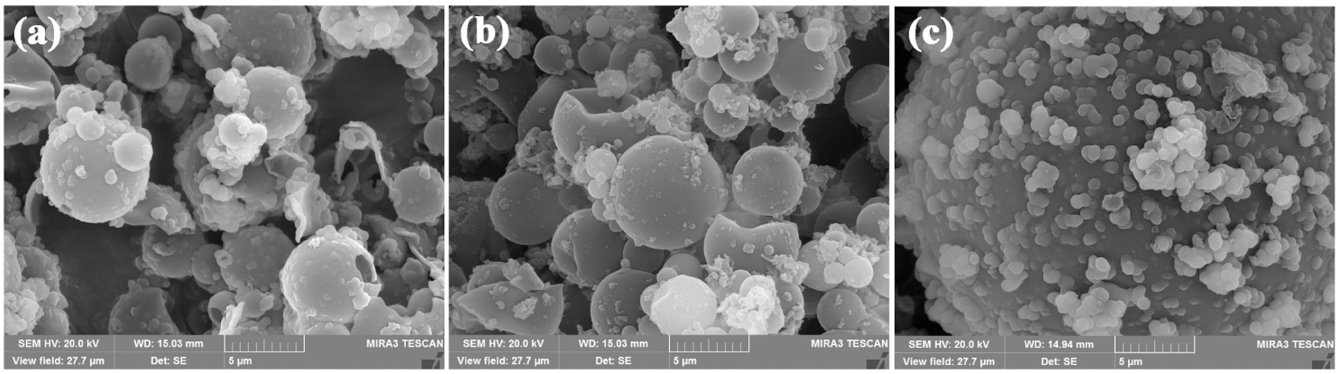

Figure 7. SEM micrographs of char residues after cone calorimeter tests of (a) pure epoxy, (b) DOPO−GO/epoxy, and (c) DOPO−VTES−GO/epoxy.

DOPO−VTES−GO/epoxy composite is much more compact than that of the DOPO−GO/epoxy composite (Figure 6d,e). The compact char layer can efficiently protect the underneath epoxy matrix from combustion by restraining the transfer of volatiles and heat through the barrier effect.

To reveal the flame-retardant mechanism, the micromorphology and elemental composition of the combusted residual chars after cone calorimeter tests were conducted by SEM−EDX, as shown in Figure 7 and Table 4. For pure epoxy, it can be obviously observed in Figure 7a that the char layer after combustion displayed a loose and porous structure. Figure 7b shows that the main component of the residue char was carbon. As shown in Figure 7c, there is a more compact structure in the residue char of DOPO−GO/epoxy. The char layer can prevent flammable gas from escaping and reduce heat transfer during the combustion process. Phosphorus was detected and oxygen contents were increased, which is because DOPO was combined with oxygen to generate phosphate compounds.[38] Also, this indicated that DOPO plays a flame-retardant role in the condensed phase. The incorporation of DOPO−VTES−GO in epoxy can further form a more compact and continuous char layer, reflecting the physical structure integrity of the char layer. Based on the previous research, there is a close relationship between flame retardancy and the structure of residual chars.[39] The compact and continuous char layer could not only reduce the transfer of combustible gas and oxygen but also have a thermal insulation effect during combustion.[40] A number of silicon elements were observed in the residual char of DOPO−VTES−GO/epoxy, which was helpful for improving the thermal stability and physical integrity of the char together with better flame retardancy.

Table 4. Elemental Compositions of the Residual Chars of Pure Epoxy, DOPO−GO/Epoxy, and DOPO−VTES−GO/Epoxy

	elemental concentration (wt %)				
sample	C	N	O	Si	P
pure epoxy	97.1	1.1	1.8		
DOPO−GO/epoxy	73.7	0.8	24.1		1.4
DOPO−VTES−GO/epoxy	53.8	0.7	40.3	4.3	0.9

Raman spectra were used to characterize the microstructure of chars, which may provide valuable information for the further study of the flame-retardant mechanism.[41] The degree of graphitization is a very important structural parameter. Figure 8 presents the Raman spectra of the residual chars of pure epoxy, DOPO−GO/epoxy, and DOPO−VTES−GO/epoxy composites after cone calorimeter tests. As shown in Figure 8a, the spectrum of pure epoxy displays two prominent peaks at 1351 cm^{-1} (disordered char) and 1585 cm^{-1} (graphite), corresponding to D and G bands, respectively. The ratio of the D and G band intensities (I_D/I_G) is inversely proportional to the in-plane crystallite sizes, which is used for estimating the graphitization degree of the residual char, and a lower I_D/I_G value means a higher degree of graphitization.[42] The I_D/I_G value of the char for pure epoxy is 2.83. Figure 8b shows a lower I_D/I_G value of 2.55 with the addition of DOPO−GO in epoxy resin. The increase of graphitization degree may be due to the catalytic charring of DOPO−GO. In addition, the I_D/I_G value of the char for the DOPO−VTES−GO/epoxy composite is 2.25. It can be reasonably concluded that DOPO−VTES−GO not only has good charring ability but also exhibits the ability to enhance the thermo-oxidative stability of the char layer, resulting in an improvement of flame retardancy performance.

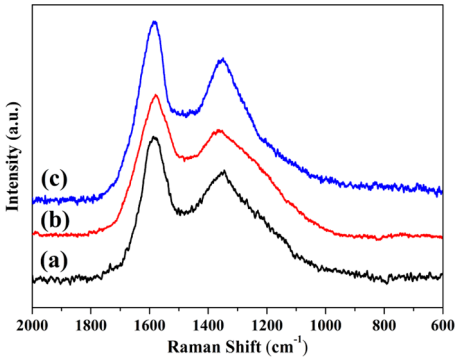

Figure 8. Raman spectra of the char residues after cone calorimeter tests of (a) pure epoxy, (b) DOPO−GO/epoxy, and (c) DOPO−VTES−GO/epoxy.

Furthermore, FTIR analysis is used to investigate the chemical structure of char residues after cone calorimeter tests for pure epoxy, DOPO−GO/epoxy, and DOPO−VTES−GO/epoxy composites, as shown in Figure 9. For the pure epoxy (Figure 9a), the absorbance peak at 1598 cm^{-1} can be ascribed to the C═C bond stretching vibration of poly-aromatic carbons.[43] Also, the peak at 1053 cm^{-1} is mainly due to the C═O groups. In the FTIR spectrum of DOPO−GO/epoxy, the polyaromatic carbon absorbance at 1598 cm^{-1} is

DOI: 10.1021/acsomega.9b00852
ACS Omega 2019, 4, 10975−10984

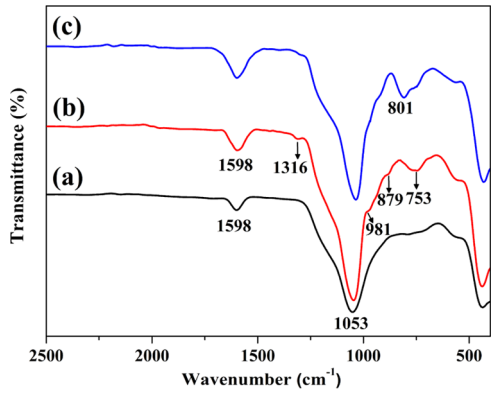

Figure 9. FTIR spectra of char residues after cone calorimeter tests of (a) pure epoxy, (b) DOPO−GO/epoxy, and (c) DOPO−VTES−GO/epoxy.

obviously enhanced, and several characteristic absorption peaks at 1316, 981, 879, and 753 cm^{-1} belong to the stretching vibrations of P═O and P−O−P structures, indicating the formation of phosphate compounds.[38] This result suggests that polyphosphoric acid was formed during thermal degradation of DOPO−GO/epoxy and promotes the formation of the carbonaceous char by carbonization. The FTIR spectrum of the DOPO−VTES−GO/epoxy composite is similar to that of DOPO−GO/epoxy, and the absorbance at 1000−1100 cm^{-1} is more obvious, which means that more Si−O−Si−O and −P(═O)−O−Si− structures remain in the char layer,[44] indicating an interaction between Si and P elements during the combustion. In addition, an absorption peak appearing at 801 cm^{-1} is caused by the Si−O−C deformation vibration and/or Si−C stretching vibration, which reveals the formation of silica compounds during the combustion.

2.5. Flame Retardancy Mechanism. Based on the above analysis, it is concluded that DOPO−VTES−GO could significantly improve the flame retardancy of epoxy resin by synergism of the catalyzing carbonization in the condensed phase and free-radical quenching in the gas phase, and a possible flame-retardant mechanism during the combustion is proposed, as shown in Figure 10. The introduction of GO can reduce the flammable gas permeability during the degradation of the epoxy molecules. In the decomposition process of DOPO groups in DOPO−VTES−GO, a phosphorus-rich residue is formed to promote the formation of char residues.[45] A continuous and compact char layer can act as an effective barrier against heat transmission and gas transport. Meanwhile,

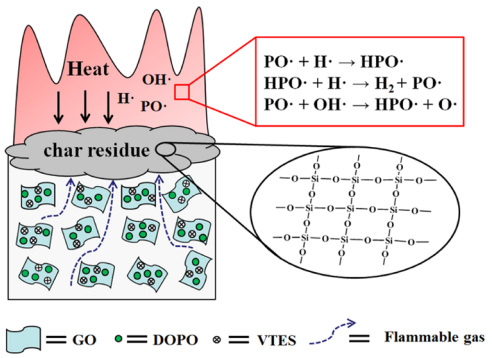

Figure 10. Possible flame-retardant mechanism during the combustion in the DOPO−VTES−GO/epoxy composite.

PO free radicals can be released during the degradation process of DOPO and capture H and OH free radicals generated by thermal decomposition of epoxy molecular chains, resulting in the chain reaction that sustains combustion to stop in the gas phase.[46] Furthermore, VTES groups in DOPO−VTES−GO tend to form the thermostable bridged structure of Si−O−Si, which promotes the formation of the graphitic structure and enhances the thermostability of char residues in the condensed phase. Therefore, DOPO−VTES−GO/epoxy composite exhibits better flame retardancy.

3. CONCLUSIONS

In this work, a novel DOPO−VTES−GO was successfully prepared via a solvothermal and hydrolysis−condensation reaction approach, which was confirmed by TEM−EDS, FTIR, and TG analyses. Then, DOPO−VTES−GO was introduced into epoxy resin through a simple solution mixing method, and the prepared DOPO−VTES−GO/epoxy composite demonstrated significant improvements in thermal stability and flame retardancy. With the incorporation of DOPO−GO and DOPO−VTES−GO, the thermal stability and flame retardancy properties of epoxy composites were improved. Compared with that of the DOPO−GO/epoxy, the char residue yield of DOPO−VTES−GO/epoxy composite was remarkably increased from 24.5 to 30.2 wt %, and the DOPO−VTES−GO/epoxy composite had a lower THR (from 59.6 to 50.5 MJ m^{-2}) and TSP (from 21.8 to 18.3 m^2). Furthermore, char residue analysis suggested that the addition of DOPO−VTES−GO exhibits an effectively synergistic effect on flame retardancy of epoxy resin by the combination of the condensed phase and gas-phase mechanism. This investigation may provide new insights into the design and synthesis of excellent flame retardants and their applications in flammable polymer materials.

4. EXPERIMENTAL SECTION

4.1. Materials. Natural flake graphite powder (purity 99.9%) with an average particle size of 500 mesh was supplied by Qingdao Xingyuan Graphite Co., Ltd. (Shandong, China). Concentrated sulfuric acid (98%), sodium nitrate, potassium permanganate, hydrogen peroxide (30%), hydrochloric acid, anhydrous ethanol, acetic acid, and acetone all were of analytical reagent grade and purchased from Chengdu Kelong Chemical Co., Ltd. (Chengdu, China). DOPO was supplied by Guangdong Wengjiang Chemical Reagent Co., Ltd. (Guangdong, China). Vinyltriethoxysilane (VTES) was kindly supplied by Qufu Chenguang Chemical Co., Ltd. (Shandong, China). Epoxy resin (E-51, epoxy value: 0.48−0.54 mol/100 g) was purchased from Hangzhou Wuhuigang Adhesive Co., Ltd. (Hangzhou, China). 4,4-Diamino-diphenyl methane (DDM) was obtained from Aladdin Industrial Corporation (Shanghai, China).

4.2. Preparation of DOPO−GO and DOPO−VTES−GO. Graphite oxide was prepared from natural flake graphite according to a modified Hummers method,[47] and thereafter, graphene oxide was obtained by ultrasonic stripping of graphite oxide. Subsequently, DOPO−GO was prepared using a simple solvothermal method. The detailed process can be described as follows. The as-prepared graphene oxide (0.1 g), DOPO (0.5 g), and anhydrous ethanol (100 mL) were mixed and sonicated for 30 min in an ultrasonic bath. After that, the solution was sealed in a 200 mL Teflon-lined autoclave and

DOI: 10.1021/acsomega.9b00852
ACS Omega 2019, 4, 10975−10984

maintained at 85 °C for 10 h. Then, the mixtures were filtered and thoroughly washed with anhydrous ethanol to remove the residual DOPO. Finally, the collected DOPO−GO was dried in a vacuum oven at 50 °C overnight to remove the solvent. Then, VTES (1 mL), deionized water (5 mL), anhydrous ethanol (150 mL), acetic acid (0.2 mL), and DOPO−GO powders (0.2 g) were introduced into a 250 mL three-necked round-bottomed flask equipped with a magnetic stirrer and a reflux condenser. After stirring for 12 h at 60 °C, a black DOPO−VTES−GO powder was obtained after washing with anhydrous ethanol and drying at 50 °C in a vacuum oven. Scheme 1 illustrates the synthesis process of the DOPO−VTES−GO flame retardant.

4.3. Preparation of DOPO−GO/Epoxy and DOPO−VTES−GO/Epoxy Composites. The DOPO−VTES−GO/epoxy composite was prepared by a solution blending method. A typical procedure to produce the epoxy composite containing 5 wt % DOPO−VTES−GO is as follows. DOPO−VTES−GO (3.0 g) was uniformly dispersed in 100 mL of acetone by 30 min of sonication, and the suspension was transferred into a 250 mL three-necked flask. Then, epoxy resins (60 g) were added into the three-necked flask under vigorous mechanical stirring and heated at 60 °C for 6 h to remove acetone. Subsequently, the curing agent DDM (20 g) was added into the three-necked flask under vigorous stirring until complete homogeneity. The mixture was poured into a preheated poly(tetrafluoroethylene) mold and cured at 120 °C for 4 h and then at 160 °C for 2 h. After curing, the sample was cooled slowly to room temperature and the DOPO−VTES−GO/epoxy composite was obtained. For comparison, pure epoxy, GO/epoxy, DOPO/epoxy, and DOPO−GO/epoxy composites were also prepared using the same method. All of the formations of pure epoxy and epoxy composites are listed in Table 1.

4.4. Characterization. TEM analyses were conducted using a JEOL JEM-2100 electron microscope with an accelerating voltage of 200 kV equipped with an EDAX energy-dispersive X-ray spectrometer (EDS, AMETEK, Mahwah), and the samples for the TEM measurements were dispersed in anhydrous ethanol under ultrasonication for 20 min and then dripped onto copper grids for tests. FTIR spectra were recorded with a resolution of 4 cm^{-1} using a Tensor 27 FTIR spectrophotometer (Bruker Company, Germany), and each sample was mixed with KBr powders and pressed into the tablet for tests. TGA was carried out using a STA 449 F5 thermoanalyzer instrument (Netzsch Company, Germany) from room temperature to 700 °C at a heating rate of 10 °C min^{-1} under a nitrogen atmosphere. The limiting oxygen index (LOI) test was carried on an HC-2 oxygen index meter (Jiangning Analysis Instrument Company, China) according to the ASTM D2863 standard method, and the specimens used were of dimensions 100 × 6.5 × 3 mm^3. Cone calorimetry tests were performed on the cone calorimeter (Fire Testing Technology, U.K.) according to ISO 5660 standard procedures, and each specimen was prepared with the dimension of 100 × 100 × 3 mm^3, mounted on an aluminum foil and irradiated horizontally at a heat flux of 35 kW m^{-2}. The morphology and composition of the char residue after cone calorimetry tests were observed using a Vega3 Tescan scanning electron microscopy (SEM) instrument with an accelerating voltage of 20 kV and energy disperse X-ray spectroscopy (EDS), and the surfaces of the samples were previously coated with a conductive layer of gold. Raman spectra were recorded using a LabRAM HR Raman spectrometer (Horiba Jobin Yvon, France) in the range of 500−2000 cm^{-1} using a laser wavelength of 632.8 nm.

AUTHOR INFORMATION

Corresponding Authors

*E-mail: quanyiliu2005@126.com (Q.L.).
*E-mail: heyuanhua@cafuc.edu.cn. Tel: +86-0838-5187202. Fax: +86-0838-5187202 (Y.H.).

ORCID

Yuanhua He: 0000-0002-1871-5923

Notes

The authors declare no competing financial interest.

ACKNOWLEDGMENTS

The authors acknowledge the financial support from the National Natural Science Foundation of China (Grant No. U1633203), the Sichuan Science and Technology Program (Grant No. 2018GZYZF0069), and the General Program of Civil Aviation Flight University of China (Grant No. J2018-07).

REFERENCES

(1) Zhang, X.; He, Q.; Gu, H.; Colorado, H. A.; Wei, S.; Guo, Z. Flame-retardant electrical conductive nanopolymers based on bisphenol F epoxy resin reinforced with nano polyanilines. *ACS Appl. Mater. Interfaces* **2013**, *5*, 898.

(2) Vijayan, P.; Hany El-Gawady, Y. M.; Al-Maadeed, M. A. S. Halloysite nanotube as multifunctional component in epoxy protective coating. *Ind. Eng. Chem. Res.* **2016**, *55*, 11186.

(3) Zeng, X.; Ye, L.; Guo, K.; Sun, R.; Xu, J.; Wong, C. P. Fibrous epoxy substrate with high thermal conductivity and low dielectric property for flexible electronics. *Adv. Electron. Mater.* **2016**, *2*, No. 1500485.

(4) Liu, T.; Zhang, L.; Chen, R.; Wang, L.; Han, B.; Meng, Y.; Li, X. Nitrogen-free tetrafunctional epoxy and its DDS-cured high-performance matrix for aerospace applications. *Ind. Eng. Chem. Res.* **2017**, *56*, 7708.

(5) Gu, H.; Ma, C.; Gu, J.; Guo, J.; Yan, X.; Huang, J.; Zhang, Q.; Guo, Z. An overview of multifunctional epoxy nanocomposites. *J. Mater. Chem. C* **2016**, *4*, 5890.

(6) Akatsuka, M.; Takezawa, Y.; Amagi, S. Influences of inorganic fillers on curing reactions of epoxy resins initiated with a boron trifluoride amine complex. *Polymer* **2001**, *42*, 3003.

(7) Hergenrother, P. M.; Thompson, C. M.; Smith, J. G., Jr.; Connell, J. W.; Hinkley, J. A.; Lyon, R. E.; Moulton, R. Flame retardant aircraft epoxy resins containing phosphorus. *Polymer* **2005**, *46*, 5012.

(8) Bourbigot, S.; Duquesne, S. Fire retardant polymers: recent developments and opportunities. *J. Mater. Chem.* **2007**, *17*, 2283.

(9) Perret, B.; Schartel, B.; Stöß, K.; Ciesielski, M.; Diederichs, J.; Döring, M.; Krämer, J.; Altstädt, V. Novel DOPO-based flame retardants in high-performance carbon fibre epoxy composites for aviation. *Eur. Polym. J.* **2011**, *47*, 1081.

(10) Wang, J.; Ma, C.; Wang, P.; Qiu, S.; Cai, W.; Hu, Y. Ultra-low phosphorus loading to achieve the superior flame retardancy of epoxy resin. *Polym. Degrad. Stab.* **2018**, *149*, 119.

(11) Liu, S.; Yan, H.; Fang, Z.; Wang, H. Effect of graphene nanosheets on morphology, thermal stability and flame retardancy of epoxy resin. *Compos. Sci. Technol.* **2014**, *90*, 40.

(12) Yu, B.; Shi, Y.; Yuan, B.; Qiu, S.; Xing, W.; Hu, W.; Song, L.; Lo, S.; Hu, Y. Enhanced thermal and flame retardant properties of flame-retardant-wrapped graphene/epoxy resin nanocomposites. *J. Mater. Chem. A* **2015**, *3*, 8034.

DOI: 10.1021/acsomega.9b00852
ACS Omega 2019, 4, 10975−10984

(13) Zhang, Y.; Yu, B.; Wang, B.; Liew, K. M.; Song, L.; Wang, C.; Hu, Y. Highly effective P−P synergy of a novel DOPO-based flame retardant for epoxy resin. *Ind. Eng. Chem. Res.* **2017**, *56*, 1245.
(14) Sun, F.; Yu, T.; Hu, C.; Li, Y. Influence of functionalized graphene by grafted phosphorus containing flame retardant on the flammability of carbon fiber/epoxy resin (CF/ER) composite. *Compos. Sci. Technol.* **2016**, *136*, 76.
(15) Liao, S. H.; Liu, P. L.; Hsiao, M. C.; Teng, C. C.; Wang, C. A.; Ger, M. D.; Chiang, C. L. One-step reduction and functionalization of graphene oxide with phosphorus-based compound to produce flame-retardant epoxy nanocomposite. *Ind. Eng. Chem. Res.* **2012**, *51*, 4573.
(16) Luo, F.; Wu, K.; Guo, H.; Zhao, Q.; Lu, M. Simultaneous reduction and surface functionalization of graphene oxide for enhancing flame retardancy and thermal conductivity of mesogenic epoxy composites. *Polym. Int.* **2017**, *66*, 98.
(17) Liu, S.; Fang, Z.; Yan, H.; Wang, H. Superior flame retardancy of epoxy resin by the combined addition of graphene nanosheets and DOPO. *RSC Adv.* **2016**, *6*, 5288.
(18) Wang, R.; Zhuo, D.; Weng, Z.; Wu, L.; Cheng, X.; Zhou, Y.; Wang, J.; Xuan, B. A novel nanosilica/graphene oxide hybrid and its flame retarding epoxy resin with simultaneously improved mechanical, thermal conductivity, and dielectric properties. *J. Mater. Chem. A* **2015**, *3*, 9826.
(19) Qian, X.; Song, L.; Yu, B.; Wang, B.; Yuan, B.; Shi, Y.; Hu, Yuan.; Yuen, R. K. Novel organic−inorganic flame retardants containing exfoliated graphene: preparation and their performance on the flame retardancy of epoxy resins. *J. Mater. Chem. A* **2013**, *1*, 6822.
(20) Abbas, S. S.; Rees, G. J.; Kelly, N. L.; Dancer, C. E. J.; Hanna, J. V.; McNally, T. Facile silane functionalization of graphene oxide. *Nanoscale* **2018**, *10*, 16231.
(21) Arkhireeva, A.; Hay, J. N. Synthesis of sub-200 nm silsesquioxane particles using a modified Stöber sol-gel route. *J. Mater. Chem* **2003**, *13*, 3122.
(22) Lee, Y.-G.; Park, J.-H.; Oh, C.; Oh, S.-G.; Kim, Y. C. Preparation of highly monodispersed hybrid silica spheres using a one-step sol−gel reaction in aqueous solution. *Langmuir* **2007**, *23*, 10875.
(23) Li, D.; Müller, M. B.; Gilje, S.; Kaner, R. B.; Wallace, G. G. Processable aqueous dispersions of graphene nanosheets. *Nat. Nanotechnol.* **2008**, *3*, 101.
(24) Wang, J.; Xu, C.; Hu, H.; Wan, L.; Chen, R.; Zheng, H.; Liu, F.; Zhang, Min.; Shang, X.; Wang, X. Synthesis, mechanical, and barrier properties of LDPE/graphene nanocomposites using vinyl triethoxysilane as a coupling agent. *J. Nanopart. Res.* **2011**, *13*, 869.
(25) Chen, C.; Shi, S.; Wang, M.; Ma, H.; Zhou, L.; Xu, J. Superhydrophobic SiO_2-based nanocomposite modified with organic groups as catalyst for selective oxidation of ethylbenzene. *J. Mater. Chem. A* **2014**, *2*, 8126.
(26) Shieh, J. Y.; Wang, C. S. Synthesis of novel flame retardant epoxy hardeners and properties of cured products. *Polymer* **2001**, *42*, 7617.
(27) Hergenrother, P. M.; Thompson, C. M.; Smith, J. G., Jr.; Connell, J. W.; Hinkley, J. A.; Lyon, R. E.; Moulton, R. Flame retardant aircraft epoxy resins containing phosphorus. *Polymer* **2005**, *46*, 5012.
(28) Gao, M.; Wu, W.; Yan, Y. Thermal degradation and flame retardancy of epoxy resins containing intumescent flame retardant. *J. Therm. Anal. Calorim.* **2009**, *95*, 605.
(29) Wang, X.; Hu, Y.; Song, L.; Xing, W.; Lu, H. Thermal degradation behaviors of epoxy resin/POSS hybrids and phosphorus−silicon synergism of flame retardancy. *J. Polym. Sci., Part B: Polym. Phys.* **2010**, *48*, 693.
(30) Schartel, B.; Hull, T. R. Development of fire-retarded materials—interpretation of cone calorimeter data. *Fire Mater.* **2007**, *31*, 327.
(31) Lee, Y. R.; Kim, S. C.; Lee, H.; Jeong, H. M.; Raghu, A. V.; Reddy, K. R.; Kim, B. K. Graphite oxides as effective fire retardants of epoxy resin. *Macromol. Res.* **2011**, *19*, 66.
(32) Zhu, H.; Xu, S. A. Synthesis and properties of rigid polyurethane foams synthesized from modified urea-formaldehyde resin. *Constr. Build. Mater.* **2019**, *202*, 718.
(33) Idumah, C. I.; Hassan, A.; Bourbigot, S. Influence of exfoliated graphene nanoplatelets on flame retardancy of kenaf flour polypropylene hybrid nanocomposites. *J. Anal. Appl. Pyrol.* **2017**, *123*, 65.
(34) Wang, S. X.; Zhao, H. B.; Rao, W. H.; Huang, S. C.; Wang, T.; Liao, W.; Wang, Y. Z. Inherently flame-retardant rigid polyurethane foams with excellent thermal insulation and mechanical properties. *Polymer* **2018**, *153*, 616.
(35) Khanal, S.; Zhang, W.; Ahmed, S.; Ali, M.; Xu, S. Effects of intumescent flame retardant system consisting of tris (2-hydroxyethyl) isocyanurate and ammonium polyphosphate on the flame retardant properties of high-density polyethylene composites. *Composites, Part A* **2018**, *112*, 444.
(36) Ronkay, F.; Molnár, B.; Szalay, F.; Nagy, D.; Bodzay, B.; Sajó, I. E.; Bocz, K. Development of flame-retarded nanocomposites from recycled PET bottles for the electronics industry. *Polymers* **2019**, *11*, 233.
(37) Qian, L.; Qiu, Y.; Sun, N.; Xu, M.; Xu, G.; Xin, F.; Chen, Y. Pyrolysis route of a novel flame retardant constructed by phosphaphenanthrene and triazine-trione groups and its flame-retardant effect on epoxy resin. *Polym. Degrad. Stabil.* **2014**, *107*, 98.
(38) Yang, S.; Wang, J.; Huo, S.; Wang, M.; Wang, J.; Zhang, B. Synergistic flame-retardant effect of expandable graphite and phosphorus-containing compounds for epoxy resin: Strong bonding of different carbon residues. *Polym. Degrad. Stabil.* **2016**, *128*, 89.
(39) Wang, X.; Song, L.; Yang, H.; Xing, W.; Kandola, B.; Hu, Y. Simultaneous reduction and surface functionalization of graphene oxide with POSS for reducing fire hazards in epoxy composites. *J. Mater. Chem.* **2012**, *22*, 22037.
(40) Schäfer, A.; Seibold, S.; Walter, O.; Döring, M. Novel high T_g flame retardancy approach for epoxy resins. *Polym. Degrad. Stabil.* **2008**, *93*, 557.
(41) Feng, C.; Liang, M.; Jiang, J.; Huang, J.; Liu, H. Synergistic effect of a novel triazine charring agent and ammonium polyphosphate on the flame retardant properties of halogen-free flame retardant polypropylene composites. *Thermochim. Acta* **2016**, *627−629*, 83.
(42) Atchudan, R.; Cha, B. G.; Lone, N.; Kim, J.; Joo, J. Synthesis of high-quality carbon nanotubes by using monodisperse spherical mesoporous silica encapsulating iron oxide nanoparticles. *Korean J. Chem. Eng.* **2019**, *36*, 157.
(43) Zhang, W.; Fina, A.; Cuttica, F.; Camino, G.; Yang, R. Blowing-out effect in flame retarding epoxy resins: insight by temperature measurements during forced combustion. *Polym. Degrad. Stab.* **2016**, *131*, 82.
(44) Zhang, W.; Li, X.; Yang, R. Study on flame retardancy of TGDDM epoxy resins loaded with DOPO-POSS compound and OPS/DOPO mixture. *Polym. Degrad. Stab.* **2014**, *99*, 118.
(45) Chiang, C. L.; Ma, C. C. M.; Wang, F. Y.; Kuan, H. C. Thermo-oxidative degradation of novel epoxy containing silicon and phosphorous nanocomposites. *Eur. Polym. J.* **2003**, *39*, 825.
(46) Ran, S.; Ye, R.; Cai, Y.; Shen, H.; He, Y.; Fang, Z.; Guo, Z. Synergistic flame retardant mechanism of lanthanum phenylphosphonate and decabromodiphenyl oxide in polycarbonate. *Polym. Compos.* **2019**, *40*, 986.
(47) Hummers, W. S., Jr.; Offeman, R. E. Preparation of graphitic oxide. *J. Am. Chem. Soc.* **1958**, *80*, No. 1339.

DOI: 10.1021/acsomega.9b00852
ACS Omega 2019, 4, 10975−10984